Available online at www.sciencedirect.com
SCIENCE DIRECT®
Polymer 44 (2003) 6051–6058
polymer
www.elsevier.com/locate/polymer

In situ observation of low molecular weight poly(ethylene oxide) crystal melting, recrystallization

Er-Qiang Chen[a*], Alexander J. Jing[b], Xing Weng[b], Ping Huang[b], Seoung-Wook Lee[b], Stephen Z.D. Cheng[a,b,*], Benjamin S. Hsiao[c], Fengji Yeh[c]

[a]*Department of Polymer Science and Engineering, College of Chemistry and Molecular Engineering, Peking University, Beijing 100871, People's Republic of China*
[b]*Department of Polymer Science, The Maurice Morton Institute of Polymer Science, The University of Akron, Akron, OH 44325-3909, USA*
[c]*The Department of Chemistry, The State University of New York at Stony Brook, Stony Brook, NY 11794-3400, USA*

Received 31 January 2003; received in revised form 8 April 2003; accepted 9 April 2003

Dedicated to Prof. Ian M. Ward on the occasion of his 75th birthday

Abstract

A low-molecular-weight poly(ethylene oxide) (PEO) fraction with a number-average molecular weight of 4250 g/mol was used to study the melting and recrystallization behaviors during heating. After complete crystallization at 46 °C, the PEO possessed almost exclusively once-folded chain [IF($n = 1$)] crystals and very few extended chain IF($n = 0$) crystals. Comparing differential scanning calorimetry heating experiments of the PEO bulk samples after crystallized at 46 °C with those further step-annealed at temperatures (T_as) in the melting range of the IF($n = 1$) crystals showed that the crystal melting and recrystallization occur to form the IF($n = 0$) crystals. In situ melting and recrystallization of the PEO crystals after crystallized at 46 °C were also investigated using both small angle X-ray scattering (SAXS) experiments in reciprocal space and atomic force microscopy (AFM) coupled with a hot stage in real space. It was found that in the SAXS measurements, the lamellar long period shifted from the IF($n = 1$) crystals towards the IF($n = 0$) crystals. This transformation process involved melting and recrystallization. During this process, more than one lamellar long period could exist. At $T_a = 58$ °C, the long period reached the thickness of the IF($n = 0$) crystals. In the in situ AFM observations, the IF($n = 1$) crystals was melted starting from inner parts of the surface lamellae, whereas the lamellar edges were quickly transformed to the IF($n = 0$) crystals with higher thermodynamic stability. The remaining lamellar edges serve as nucleation sites of the PEO recrystallization. The IF($n = 0$) crystal growth rate measured by the in situ AFM was slower than that measured in the single crystals of the isothermal crystallization at the same temperature. The fast overall recrystallization of the IF($n = 0$) crystals was mainly deduced by the fact that the high nucleation density provided by the survived nucleation sits such as the lamellar edges.

Keywords: Annealing; Recrystallization; Crystal melting

1. Introduction

In the past, two sets of experimental observations were extensively reported on the crystal growth in the melt, crystal morphology, annealing and melting of low-molecular-weight (LMW) poly(ethylene oxide) (PEO) factions. One set was based on the observations of single crystals of LMW PEOs and another set, for the bulk samples. All the structural and morphological studies for PEO single crystals revealed that the lamellar crystal thickness increases quantizely due to their integral numbers of chain folding (IF), such as the extended chain [IF($n = 0$)] crystal, the once-folded chain [IF($n = 1$)] crystal, the twice-folded chain [IF($n = 2$)] crystal, etc. under polarized light microscopy (PLM) [1–5]. The shape of single crystals changes with respect to the undercooling (ΔT) in the high crystallization temperature (T_c) region. Generally speaking, the single crystals are facetted. However, in the vicinity of

* Corresponding author. Address: Department of Polymer Science, The Maurice Morton Institute of Polymer Science, The University of Akron, Akron, OH 44325-3909, USA. Tel.: +1-330-972-6931; fax: +1-330-972-8626.
E-mail addresses: cheng@polymer.uakron.edu (S.Z.D. Cheng), scheng@uakron.edu (S.Z.D. Cheng), eqchen@pku.edu.cn (E.Q. Chen).

0032-3861/03/$ - see front matter © 2003 Published by Elsevier Ltd.
doi:10.1016/S0032-3861(03)00557-3

the transition temperatures between the IF(n) and IF($n-1$) crystals, those single crystals may also be rounded [2–6]. The isothermal thickening of the single crystals during annealing can be clearly observed by the transformation of the fold number of n to $n-1$, and it starts at the center of the single crystal [2–5].

On the other hand, crystallization of the bulk LMW PEO fractions provided evidence of non-integral folding (NIF) crystals as an initiate transient state [6–12], similar to the cases of n-alkins [13,14]. Although this NIF crystal was also responsible to the single crystal growth, the limited resolution of PLM prevented the observation of this NIF crystal. It is now known that the IF crystals in PEO are generated from the NIF crystals via the thickening and thinning processes during the isothermal annealing. An unanswered question is how the crystal melting, recrystallization and thickening take place during heating in the bulk LMW PEO samples. It is speculated that for example, the thickening process in the bulk has to be different from that in the single crystals due to different environments during annealing. In the single crystal, it is surrounded by the PEO melt and the crystal thickening can be readily taken place by pulling the liquid PEO molecules surrounded into the crystal. The number of PEO molecules in this crystal thus increases. The thickening process is always initiated at the center of the crystal, which was formed the earliest. However, in the bulk PEO samples molecular mechanism of this process is less understood, and the crystals are in the form of multiple lamellar stacking. Any lamellar thickening needs to overcome the neighboring lamellar confinements, and thus, it requires a cooperative thickening process. Furthermore, no free liquid PEO molecules available between neighboring lamellae. It is conceivable that the lamellar thickening may start from the less confined locations instead of the center of each lamella. Moreover, a thickness increase in the bulk crystals has also to be thermodynamically balanced by creating new lateral surfaces, since the overall number of PEO molecules involved in this process is constant.

In order to clearly identify the different behaviors of the bulk lamellar crystals in melting and recrystallization during annealing from those of the LMW PEO single crystals, in this publication, we intend to utilize different experimental techniques to monitor these behaviors in a PEO fraction with a number-average molecular weight (M_n) of 4250 g/mol. This includes differential scanning calorimetry (DSC), in situ synchrotron small angle X-ray scattering (SAXS) and observations of atomic force microscopy (AFM) coupled with a hot stage. DSC experiments provide heat absorption and releasing during the first-order transition processes, while SAXS results give rise to PEO lamellar long period changes with different annealing temperatures (T_a) and times (t_a). The in situ AFM technique monitors surface morphological changes in the melting and recrystallization of PEO bulk lamellar crystals.

2. Experimental section

2.1. Materials and sample preparations

The PEO with M_n of 4250 g/mol was purchased from Polymer Laboratory, Ltd. The polydespersity is 1.03 after refractionation in our laboratory. Gel permeation chromatography calibrated by PEO standards was used to determine the molecular weight distribution for the PEO in tetrahydrofuran (THF) at 25 °C. A bulk film with a thickness of 0.5 mm was melt-pressed for the samples in DSC and SAXS measurements. For the AFM experiments, the PEO thin film was cast from a chloroform solution of 5% (w/v) to carbon coated cover glass slide surface. After drying in vacuum for overnight, the sample was mounted to the AFM hot stage and protected by the purge gas of dry nitrogen. The sample thickness was around 0.1 mm.

2.2. Experiments and equipment

DSC experiments (TA2100) was used to carry out the isothermal crystallization, and monitor the melting and recrystallization in the melting region of the IF($n=1$) crystals of the PEO. The DSC was calibrated using indium and other standard materials. Isothermal crystallization of the PEO was carried out by quenching the PEO melt to the isothermal T_c at 46 °C. A 30 min isothermal time (t_c) was enough to ensure the complete crystallization and develop the IF($n=1$) crystals. The melting and recrystallization behaviors of the PEO crystals formed at 46 °C was examined by directly heating the sample from the T_c to annealing temperatures ($T_a = 53.5$, 54.5 and 56.5 °C), and sequentially annealed the sample at each temperature for a period of time ($t_a = 30$ min). The annealed samples were then directly heated to 70 °C, and the melting traces were recorded at a heating rate of 5 °C/min.

Measurements of synchrotron SAXS were performed at the synchrotron X-ray beam line 27C of the National Synchrotron Light Source at Brookhaven National Laboratory. The wavelength of the X-ray beam was 0.1307 nm. A position-sensitive proportional counter was used to record scattering patterns. The counter was calibrated with a duck tendon giving scattering peaks at the scattering vector q of 0.0109, 0.022, 0.033 nm^{-1}, etc. ($q = 4\pi\sin\theta/\lambda$, where λ is the wavelength of the X-ray radiation). Isothermal crystallization and annealing measurements were made on a customized two-chamber hot stage. The temperature was controlled within ±0.5 °C. The PEO sample was first quenched to $T_c = 46$ °C from the melt, and kept there at 30 min duration. The SAXS data were recorded at that temperature. The sample was then isothermal annealed at different temperatures ($T_a = 51$, 52, 53 °C for 3 min each, 54 and 56 °C for 15 min each, and at $T_a = 58$ °C for 2 h). The SAXS data were again recorded at each temperature. For the data treatment, Lorentz correction was conducted by multiplying the intensity, I (counts per second), by q [6].

AFM (Digital Instrument, NanoScope IIIa) coupled with a hot stage was employed to study the morphology of the PEO crystals. The tapping mode of AFM was selected to obtain both height and phase images. The force used by the cantilever was light enough to avoid damaging the sample, yet it was strong enough to obtain accurate surface features. The scanning rate was 1 Hz for the scan size of 10 μm, and the resolution was 256 × 256. The operation and resonance frequencies were ~280 kHz, while the free and set point amplitudes were 43.2 mV and 2.0 V, respectively. The scanner was calibrated with the standard grid in both lateral size and height. The AFM was thus enabled to observe the surface morphology change of the PEO bulk crystals upon heating and annealing. The temperature of the hot stage manufactured by Digital Instrument was calibrated with standard materials, and controlled within ±0.5 °C using standard organic materials of *p*-nitrotoluene, naphthalate and benzoic acid. The melting temperatures of these standard materials were determined by the tapping mode of the AFM at which the materials exhibited sudden changes to the fluidity. The sample thicknesses of the standard materials were identical to that of the PEO sample. The PEO bulk sample was prepared via a concentrated PEO solution in anhydrous toluene. The PEO samples were first crystallized at 46 °C for 30 min and then, heated to a preset T_a at 53 °C for 5 min, 56 °C for 20 min and then 58 °C for 20 min. The AFM images were recorded when the sample was held isothermally at different temperatures. The growth rates at 58 °C were measured directly on the in situ images using an impurity particle as a reference (which does not affected by the heating and annealing process).

3. Results and discussion

3.1. Isothermal crystallization and annealing behaviors

It is found that for this LMW PEO(M_n = 4250), both of the IF(n = 0) and IF(n = 1) crystals may form, which are dependent upon the ΔT and t_c. We specifically choose the samples isothermally crystallized at T_c = 46 °C for the further annealing investigation, since at this temperature the bulk PEO crystals are in the almost exclusively IF(n = 1) crystals. After completing the crystallization at 46 °C for 30 min, the bulk PEO crystals are monitored to observe the IF(n = 1) crystal melting and recrystallization into the more stable IF(n = 0) crystals during heating in both reciprocal and real spaces.

Fig. 1(a) shows a DSC heating diagram of the PEO crystals after a complete crystallization (for t_c = 30 min.) at 46 °C. During heating, two melting endothermic processes are observed at peak melting temperatures (T_ms) of 57 and 60 °C, respectively. The onset T_m is usually 1–1.5 °C lower than the peak T_m. The low T_m endotherm has a major portion of the transition enthalpy with a starting T_m of 53 °C. A minor portion of the transition enthalpy at higher

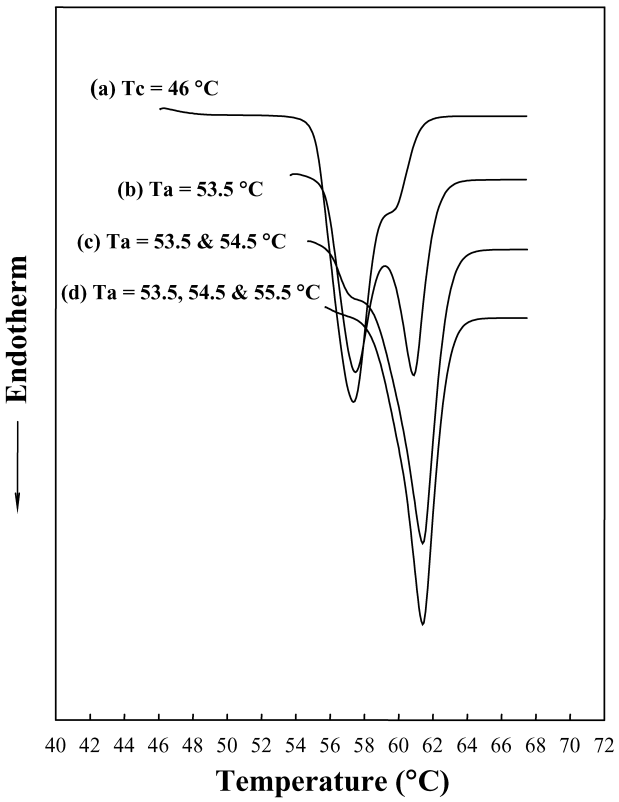

Fig. 1. DSC melting traces of PEO(M_n = 4250) : after crystallization at 46 °C (a), and annealed at 53.5 °C (b), 53.5 °C and then 54.5 °C (c), 53.5, 54.5 and then 55.5 °C for 30 min each after crystallization at 46 °C.

temperatures is attributed to the crystals which are undergoing to form the imperfect IF(n = 0) crystals (see below).

Fig. 1(b)–(d) shows the DSC heating diagrams of the PEO bulk samples which were crystallized first at 46 °C and then, were gone through the sequential annealing at different T_as for t_a = 30 min each. The T_as are specifically chosen to be higher than the onset T_m of 53.0 °C of the IF(n = 1) crystals. Therefore, the PEO crystals undergo a partial melting during the annealing. As shown in these figures, the high T_m peak temperature is slightly increased with increasing T_a, and finally, it is at 61.4 °C at T_a = 55.5 °C as shown in Fig. 1(d), which represents the T_m of the imperfect IF(n = 0) crystals. The transition enthalpy is gradually enhanced with increasing T_a. This reflects that recrystallization takes place during the annealing. When T_a is further penetrating into the melting region of the IF(n = 1) crystals, the melting and recrystallization processes during the transformation of the IF(n = 1) → IF(n = 0) crystals becomes increasingly dominant. Compared with the slow isothermal crystallization kinetics of the PEO crystals at such high temperatures (T_c > 55 °C), the recrystallization process takes place rather faster [9]. For example, after only annealed at 55.5 °C for 30 min, a single melting endotherm represented by ~80% crystallinity (based on its transition enthalpy data) of the imperfect IF(n = 0) crystals is observed. Note that the equilibrium melting temperature of the IF(n = 0) crystals of PEO(M_n =

4250) has an onset T_m of 61.0 °C (this leads to a peak temperature of 62–63.5 °C observed in the DSC experiments).

3.2. Structural evolution during isothermal annealing

Fig. 2(a) shows a set of synchrotron SAXS results of the PEO crystallization at T_c of 46 °C after a $t_c = 30$ min. The initial transient NIF crystals have been transformed to the IF($n = 1$) crystals with a long period of 13.9 nm ($q = 0.45\ nm^{-1}$, note that an average stem length of the IF($n = 1$) crystal is 13.4 nm [9]). There is also few crystals with a larger long period formed at this temperature, evidenced by a very weak scattering peak at a position of $q = 0.30\ nm^{-1}$. This long period corresponds the crystals which are undergoing a transformation to form the imperfect IF($n = 0$) crystals. This observation is consistent with the DSC observation in Fig. 1(a), although in Fig. 1(a), parts of this crystal may also be formed during heating. When the temperature is increased to $T_a = 51$ °C, the SAXS result does not have a significant change in both the q and the relative invariant values compared with those at 46 °C (Fig. 2(b)). At $T_a = 52$ °C, the main SAXS scattering peak is slightly shifted to a lower q value (see Fig. 2(c)), but its relative invariant is little changed with respect to those shown in Fig. 2(a),(b).

However, at $T_a = 53$ °C, the SAXS pattern in Fig. 2(d) starts to show some changes. Two scattering peaks can be clearly observed at the q values of 0. 33 and 0.43 nm^{-1}, respectively. These two scattering peaks are substantially broadened compared with that at lower T_as. This indicates that most of the IF($n = 1$) crystals are undergoing a transformation to form the transient crystals with thicker long periods. Two populations of the crystals with different long periods correspond to the two melting endothermic processes observed in DSC (Fig. 1(b)), and thus, two different metastabilities [15,16]. At $T_a = 54$ °C, two broad scattering peaks are further move towards lower q values (0. 29 and 0.38 nm^{-1}) as shown Fig. 2(e). The relative invariant slightly decreases in both Fig. 2(d),(e), reflects a partially melting process does occur.

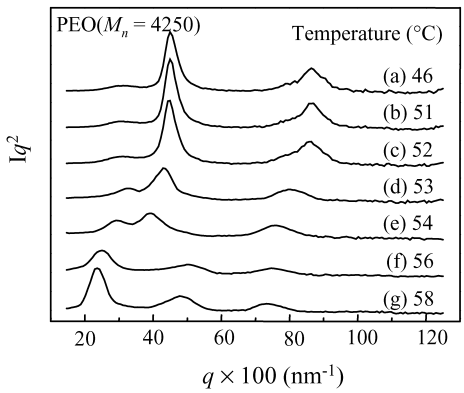

Fig. 2. Set of SAXS patterns PEO($M_n = 4250$) : after crystallization at 46 °C (a), and annealed at 53 °C (b), 54 °C (c), 56 °C for 15 min each after crystallization at 46 °C, and (d) at 58 °C for 2 h after crystallization at 46 °C.

When the T_a reaches 56 °C for 30 min in Fig. 2(f), the scattering peak moves to $q = 0.24\ nm^{-1}$, and it is a single scattering peak with its higher order scattering although the width at half-height of this scattering peak is still relatively broad, indicating that the IF($n = 0$) crystals are almost reached. This is in agreement with the DSC result as shown in Fig. 1(d). After the temperature reaches 58 °C and the sample was kept for a prolonged period of time (2 h), The single scattering peak appeared at a $q = 0.23\ nm^{-1}$, which corresponds to a long period of 27.3 nm. This is the representative of the extended IF($n = 0$) crystals (Fig. 2(g)). The relative invariant is still smaller than those at the lower T_as between 46 and 52 °C, indicating that the growth of the IF($n = 0$) crystals are not yet completed.

3.3. In situ morphological observations of crystal melting and recrystallization

Recently, polymer isothermal crystallization in single crystals [17–19], spherulites [20,21] and other crystalline morphologies [22–24] can be followed by in situ AFM technique. Fig. 3 shows a set of successive AFM surface morphologies of the PEO bulk sample during heating after the isothermal crystallization at 46 °C for 30 min. In order to clearly exhibit the lamellar morphology, both the top view (in the left column) and the view from a selected viewing angle (in the right column) are presented. Fig. 3(a) shows an AFM micrograph of the stacked PEO lamellar crystals formed at 46 °C. Each lamellar surface is relatively smooth, and they are clearly bounded by the edges. Some particles (most likely caused by impurities) are on the lamellar surfaces, and we use them as reference markers for measurements of the crystal growth rates (see below). The stacked lamellar crystals are formed most likely due to screw dislocations on the way to construct spherulites [25]. Since the sample in Fig. 3(a) was completely crystallized, this figure also serves as an internal reference for the structural height for Fig. 3(b)–(g).

The crystal starts to melt when the temperature reaches 53 °C (see Fig. 3(b)), which agrees with the DSC and SAXS observations (see Figs. 1(a) and 2(d)). Surprisingly enough, in this figure, the melting of the IF($n = 1$) crystals starts at the inner part of the top lamella (see the arrow in Fig. 3(b)), where the crystals are least stable. The height of the melt portion becomes lower than the crystal edge, which must be associated with the thickening of the edges and diffusion of the melted PEO molecules. This observation is different from the usual observations of which the melting process starts at the crystal edge [3–5]. The reason of this phenomenon may be due partially to the fact that thickening at the edges creates less new crystal surfaces compared with that taken place at the inner locations of the lamella when the number of PEO molecules in the system is constant.

The melting is progressing upon further increasing the

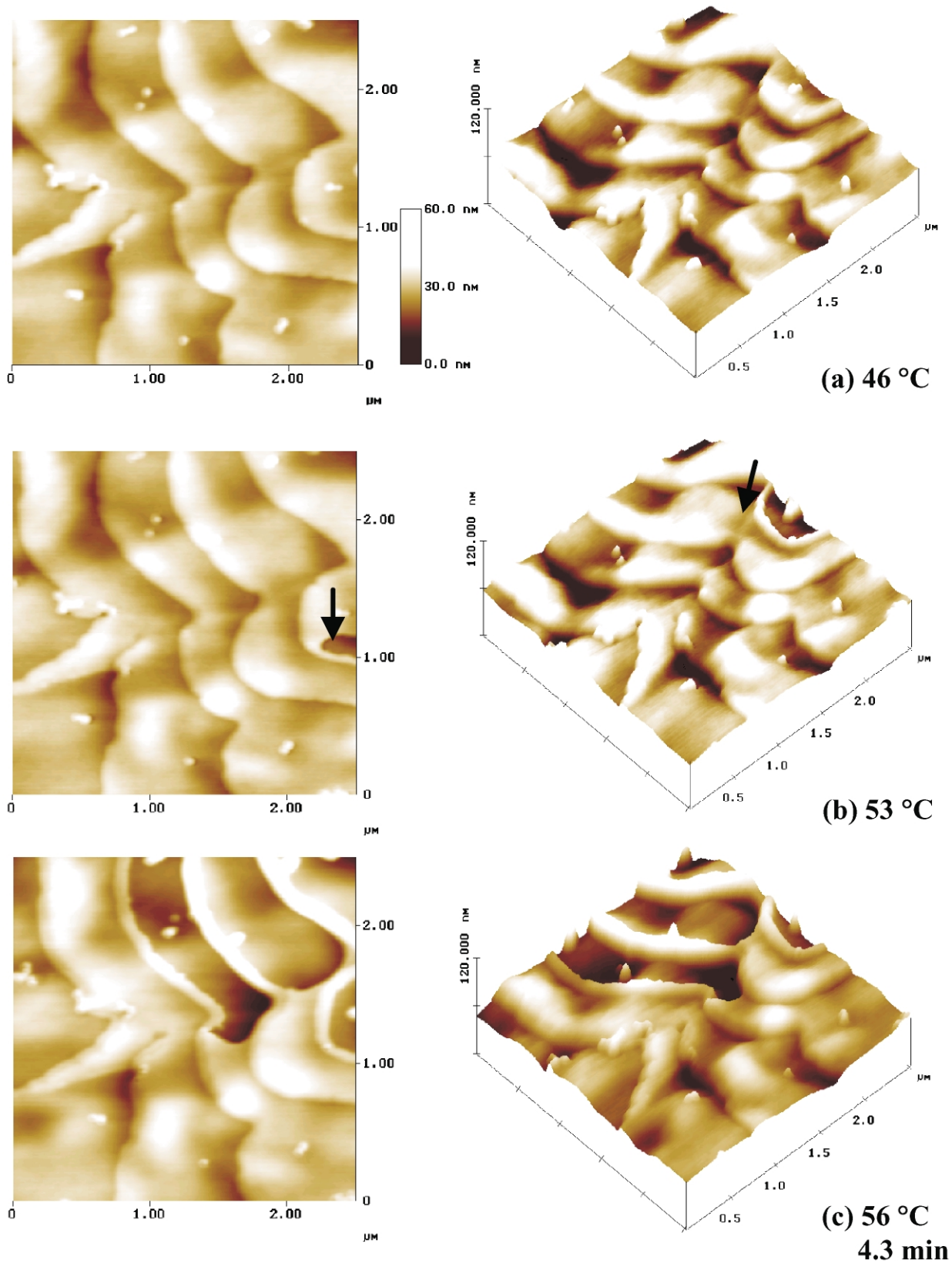

Fig. 3. Successive AFM observations (the height images) of PEO(M_n = 4250) after crystallization at 46 °C: (a) 46 °C; (b) 53 °C; (c) 56 °C (4.3 min); (d) 56 °C (8.5 min); (e) 56 °C (17.1 min); (f) 57 °C (8.5 min); (g) 57 °C (17.1 min).

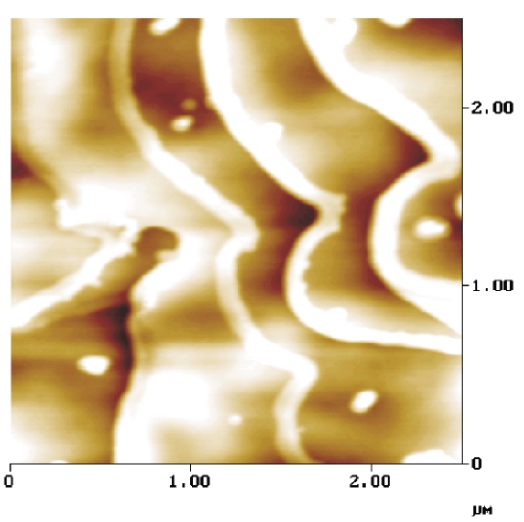

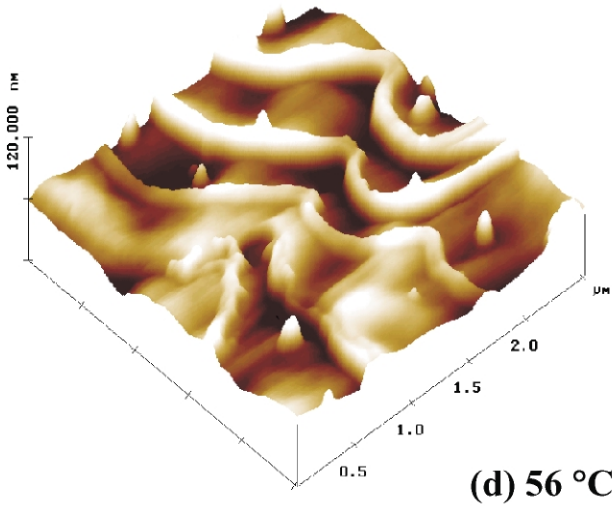

(d) 56 °C
8.5 min

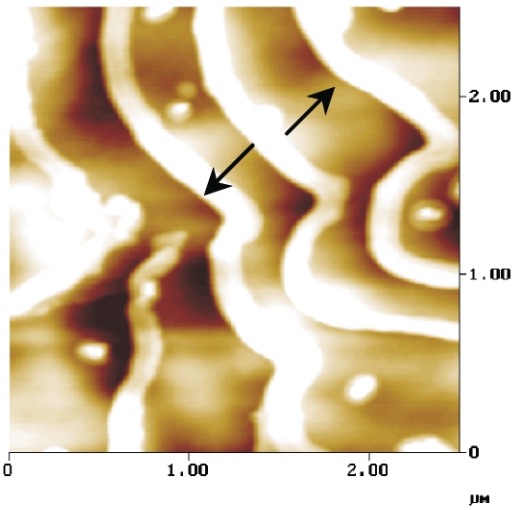

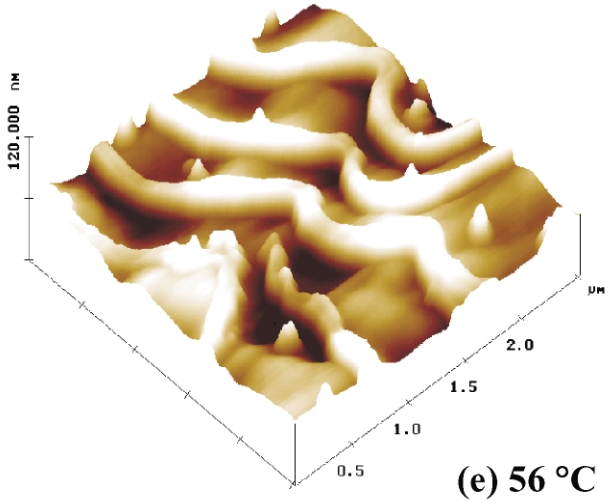

(e) 56 °C
17.1 min

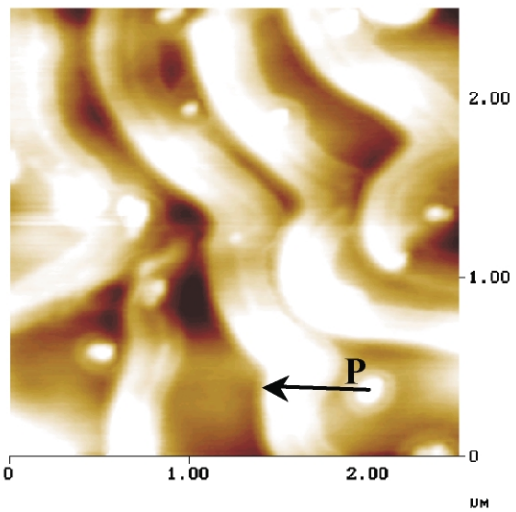

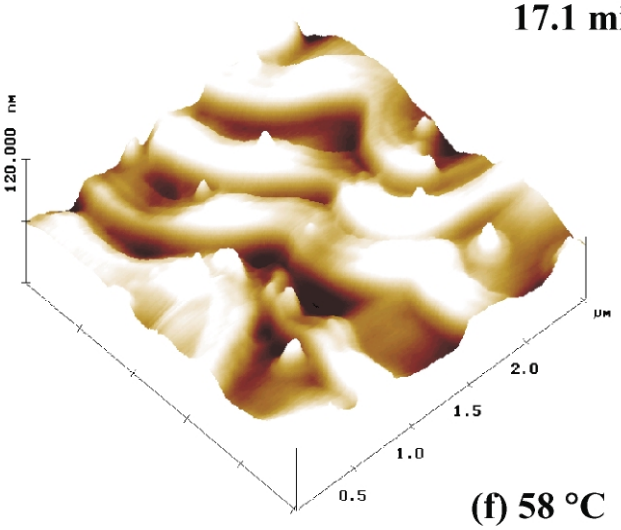

(f) 58 °C
8.5 min

Fig. 3 (*continued*)

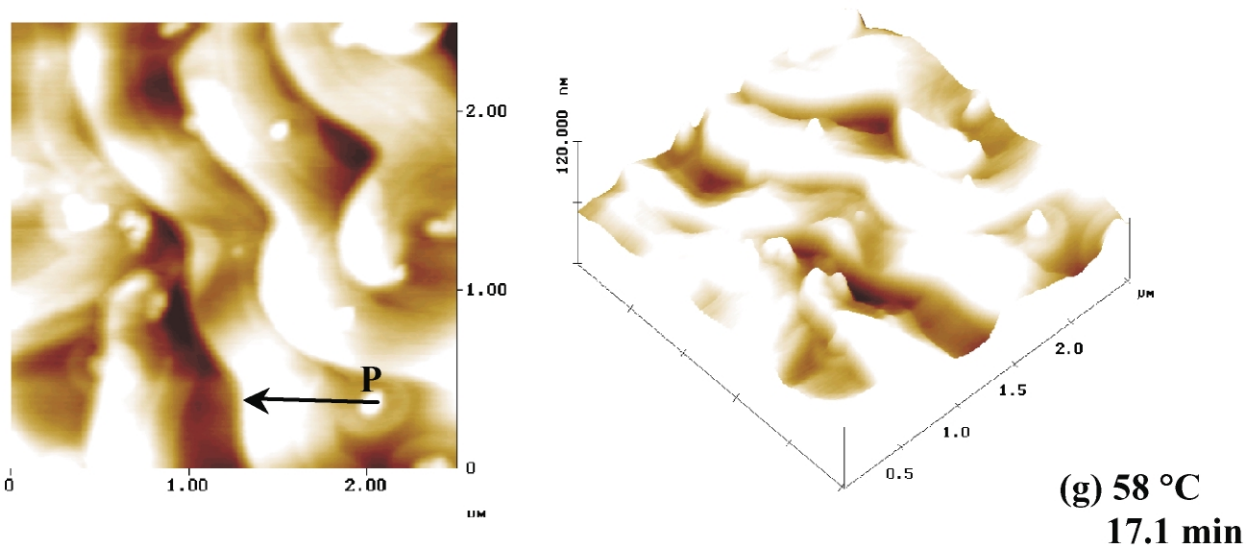

Fig. 3 (*continued*)

temperature to 56 °C as shown in Fig. 3(c)–(e). These figures are at the same T_a but for different t_as (4.3, 8.5, and 17.1 min, respectively). As shown in Fig. 3(c), the lamellar edges remain during the melting of the IF($n = 1$) crystals. The thickness of these edges increases with increasing the t_a, and finally, reaches the height of the IF($n = 0$) crystals (the thickness of ~28 nm in Fig. 3(e)). Therefore, the IF($n = 0$) crystals first appear around the edges of the lamellae. This indicates that again, crystals at the edges are easier to be annealed into the more stable IF($n = 0$) crystals.

Fig. 3(e) also shows PEO recrystallization. It can be evidenced by an increase of the width of the remaining crystal edges of the IF($n = 0$) crystals along the two opposite directions (see arrows in Fig. 3(e)). This recrystallization continuously proceeds at a higher temperature of 58 °C as shown in Fig. 3(f),(g) when the sample held there for 8.5 and 17.0 min, respectively. Comparing these two figures, it can be found that the growth of the thick edges continues. Since the IF($n = 0$) crystals possess a thickness which is double of the thickness of the IF($n = 1$) crystals, yet the number of PEO molecules in the sample remains constant, the lamellar crystal development stops soon or later. Some holes are formed in which no crystals exist. It is also conceivable that the recrystallization may not only consume the molten PEO molecules within the original layer, but also reel in the PEO molecules which originally belong to the underneath layer.

Quantitatively, the growth rate of the PEO crystals at 58 °C may be estimated in Fig. 3(f),(g). Taking the particle *P* as a reference, one can measure the distance from *P* to the front line of the lamellar edge along the direction as pointed by the arrow (see Fig. 3(f),(g)). Assuming that the growth rate is linear in this relatively small time interval (8.5 min), it is calculated to be 0.24 nm/s. Furthermore, we can compare this growth rate with that observed in the single crystal growth. By applying the self-seeding and self-decoration method [2], the linear growth rate of the PEO($M_n = 4250$) at 58 °C was measured to be 0.8 nm/s [26], which is about 3.3 times of the rate measured here by AFM in Fig. 3(f),(g). The reason may lie on the fact that the growth in those single crystals in the melt can receive the supply of surrounding liquid PEO molecules; while in this case there is no such supply. Moreover, the growth rate may not be linear in a long time interval due to the exhaustion of melted PEO molecules. On the other hand, the DSC annealing experiments in Fig. 1 reveals that the overall recrystallization is faster compared to directly crystallized sample from the melt. Therefore, one can conclude that in the bulk PEO case, the high nucleation density is the dominant factor that accelerates the recrystallization process. As shown in Fig. 3, the surviving crystals such as the edges serve as nucleation sites for the growth of the IF($n = 0$) crystal during annealing.

A recently published work reported that the crystal melting process of a very high-molecular-weight (HMW) PEO with a M_W of 2,000,000 g/mol was not explained by a mechanism of crystal melting-recrystallization or crystal thickening [27]. In our case, the LMW PEO sample possesses a M_n of 4,250 g/mol. Note that this PEO sample can be crystallized into two distinct forms: the IF($n = 0$) and the IF($n = 1$) crystals with distinct thermodynamic stabilities. Therefore, when the IF($N = 1$) crystals melt, they can be recrystallized into the IF($n = 0$) crystals. In the PEO sample with a very HMW of 2,000,000 g/mol, entanglements play an important role and no IF crystals can be formed. Therefore, the crystals in this sample do not have characteristic thermodynamic stability differences as in the case of the IF($n = 0$) and the IF($n = 1$) crystals in the low M_W PEO sample. The melting of the crystals of this very HMW sample thus show a broad endothermic process

and recrystallization (or thickening) may be suppressed due to slow crystallization rates.

4. Conclusion

Melting and recrystallization of the PEO($M_n = 4250$) samples after crystallized at $T_c = 46\,^{\circ}C$ have been examined by DSC, SAXS and AFM coupled with a hot stage. The DSC experimental results show that the melting of the IF($n = 1$) crystals and the formation of the IF($n = 0$) crystals are observed at different T_as and t_as. The recrystallization occurs rapidly when the PEO is annealed at the T_as in the melting region of the IF($n = 1$) crystals. The SAXS data express changes of the lamellar long periods with annealing conditions. The decrease of relative invariant indicates the melting of the original IF($n = 1$) crystals in the sample. A recrystallization of the IF($n = 0$) crystals is evidenced via the appearance of the q value of $0.23\,nm^{-1}$, which corresponds to a full length of the PEO($M_n = 4250$) molecules. The in situ AFM experiments provide direct observations of the melting of the IF($n = 1$) crystals. The melting takes place in the inner locations of surface lamellae, and the lamellar edges are rapidly thickened into the IF($n = 0$) crystals during annealing. Recrystallization at both sides of the survived lamellar edges is also observed. The growth rate of the IF($n = 0$) crystals in a short time interval is slower compared with that of the single crystal growth at the same temperature. Therefore, the faster overall recrystallization is due mainly to that the existed crystal edges which provide a high density of nucleation sites for the IF($n = 0$) crystal growth. This study provides the merits in two folds. First, we can clearly identify the different melting and recrystallization behaviors between the bulk lamellar crystals and single crystals in the LMW PEO fractions. Second, we may extend our knowledge to understand mechanisms of polymer crystal melting and recrystallization in different molecular weights.

Acknowledgements

This research was supported by the National Science Foundation (DMR-0203994). The author EQC also would like to acknowledge the support from National Natural Science Foundation of China (NSFC-20025414) that makes this work completed.

References

[1] Arlie JP, Spegt P, Skoulios A. Makromol Chem 1967;104:212.
[2] Kovacs AJ, Gonthier A. Colloid Polym Sci 1972;250:530.
[3] Kovacs AJ, Gonthier A, Straupe C. J Polym Sci Polym Symp 1975;50:283.
[4] Kovacs AJ, Straupe C, Gonthier A. J Polym Sci Polym Symp 1977;59:31.
[5] Kovacs AJ, Straupe C. Faraday Discuss Chem Soc 1979;68:225.
[6] Cheng SZD, Zhang AQ, Chen J-H. J Polym Sci Polym Lett Ed 1990;28:233.
[7] Cheng SZD, Zhang AQ, Chen JH, Heberer DP. J Polym Sci Polym Phys Ed 1991;287.
[8] Cheng SZD, Chen JH, Zhang AQ, Heberer DP. J Polym Sci Polym Phys Ed 1991;29:299.
[9] Cheng SZD, Zhang A, Barley JS, Chen JH, Habenschuss A, Zschack PR. Macromolecules 1991;24:3937.
[10] Cheng SZD, Chen JH, Zhang AQ, Barley JS, Habenschuss A, Zschack PR. Polymer 1992;33:1140.
[11] Cheng SZD, Chen JH, Zhang AQ, Barley JS, Habenschuss A, Zschack PR. Macromolecules 1992;25:1453.
[12] Cheng SZD, Wu SS, Chen JH, Zhuo Q, Quirk RP, von Meerwall ED, Hsiao BS, Habenschuss A, Zschack PR. Macromolecules 1993;26:5105.
[13] Ungar G, Keller A. Polymer 1986;27:1835.
[14] Ungar G, Keller A. Polymer 1987;28:1899.
[15] Keller A, Cheng SZD. Polymer 1998;39:4461.
[16] Cheng SZD, Keller A. Ann Mater Sci 1998;28:533.
[17] Magonov SN, Whangbo MH. Surface analysis with STM and AFM. Weinheim: VCH; 1996.
[18] Pearce R, Vancso GJ. Macromolecules 1997;30:5843.
[19] Zhou WS, Cheng SZD, Putthanarat S, Eby RK, Reneker DH, Lotz B, Magonov S, Hsieh ET, Geerts RG, Palackal SJ, Hawley GR, Welch MB. Macromolecules 2000;33:6861.
[20] Schultz JM, Miles MJ. J Polym Sci Part B: Polym Phys 1998;36:2311.
[21] Ivanov DA, Jonas AM. Macromolecules 1998;31:4546.
[22] Hobbs JK, McMaster TJ, Miles MJ, Barham PJ. Polymer 1998;39:2437.
[23] Godovsky YK, magonov SN. Langmuir 2000;16:3547.
[24] Basire C, Ivanov DA. Phys Rev Lett 2000;85:5587.
[25] Cheng SZD, Barley JS, GiustiI PA. Polymer 1990;31:845.
[26] Chen JH. PhD Dissertation, Department of Polymer Science, The University of Akron, 1992.
[27] Beekmans LGM, van der Meer DW, Vancso GJ. Polymer 2002;43:1887.